

Cross-species transcriptomics uncovers genes underlying genetic accommodation of developmental plasticity in spadefoot toads

Hans Christoph Liedtke¹ | Ewan Harney² | Ivan Gomez-Mestre¹ 

¹Ecology, Evolution and Development Group, Department of Wetland Ecology, Estación Biológica de Doñana, CSIC, Seville, Spain

²Department of Evolution, Ecology and Behaviour, Institute of Infection, Veterinary & Ecological Sciences, University of Liverpool, Liverpool, UK

Correspondence

Ivan Gomez-Mestre, Ecology, Evolution and Development Group, Department of Wetland Ecology, Estación Biológica de Doñana (CSIC), 41092 Sevilla, Spain.
 Email: igmestre@ebd.csic.es

Funding information

Ministerio de Economía, Industria y Competitividad (MINECO), Grant/Award Number: CGL2017-83407-P

Abstract

That hardcoded genomes can manifest as plastic phenotypes responding to environmental perturbations is a fascinating feature of living organisms. How such developmental plasticity is regulated at the molecular level is beginning to be uncovered aided by the development of -omic techniques. Here, we compare the transcriptome-wide responses of two species of spadefoot toads with differing capacity for developmental acceleration of their larvae in the face of a shared environmental risk: pond drying. By comparing gene expression profiles over time and performing cross-species network analyses, we identified orthologues and functional gene pathways whose environmental sensitivity in expression have diverged between species. Genes related to lipid, cholesterol and steroid biosynthesis and metabolism make up most of a module of genes environmentally responsive in one species, but canalized in the other. The evolutionary changes in the regulation of the genes identified through these analyses may have been key in the genetic accommodation of developmental plasticity in this system.

KEY WORDS

network analysis, *Pelobates cultripes*, RNA-Seq, *Scaphiopus couchii*, WGCNA

1 | INTRODUCTION

Adaptive phenotypic plasticity is a common feature of biological organisms that allows a given genotype to appropriately express alternative phenotypes under different environmental conditions (Schlichting & Pigliucci, 1998; West-Eberhard, 2003). The genetic regulation of such plasticity can diverge under selection in contrasting environments, resulting in evolved differences across lineages in their degree of responsiveness to environmental variation (Casas & Moczek, 2018; Schlichting & Wund, 2014; West-Eberhard, 2003).

Environmental heterogeneity is the norm in nature, and developmental processes can either be responsive or resistant to such environmental fluctuations. The evolution of developmental responses to environmental factors therefore must vary along this

gradient between plasticity and robustness (Lafuente & Beldade, 2019; Schwab et al., 2019). Adaptive plasticity evolves readily in organisms exposed to environmental heterogeneity given reliable cues to assess the environment, capitalizing on the modularity of development (Londe et al., 2015; Moczek, 2010) and its underlying regulatory gene networks (Projecto-Garcia et al., 2019; Schneider et al., 2014; Snell-Rood et al., 2009). During transitional phases to a novel or different environment, plasticity increases the viability and persistence of populations, contributing to the maintenance of genetic variability due to both simple demographic effects and to the shielding of genotypic variants from selection (Draghi & Whitlock, 2012; Gomez-Mestre & Jovani, 2013). If different plastic lineages (species or populations) experience consistently divergent environmental conditions, they can evolve differences in the environmental

sensitivity of the regulation of adaptive traits (i.e., experience genetic accommodation; West-Eberhard, 2003). Trait plasticity can therefore increase or decrease, and even be lost if organisms are exposed to stable environments for long enough (Kulkarni et al., 2011; Pigliucci et al., 2006; Suzuki & Nijhout, 2006). Such reduction in environmental sensitivity and increased developmental robustness may be achieved through a variety of mechanisms (Lafuente & Beldade, 2019), such as redundancy in gene enhancers (Frankel et al., 2010) and regulatory microRNAs (Brenner et al., 2010).

Environmentally induced changes in development often result from environmentally induced changes in gene expression (Beldade et al., 2011; Lafuente & Beldade, 2019). Consequently, a promising approach to the study of genetic accommodation is to compare the environmental sensitivity in gene expression of species or populations with divergent responses to standardized environmental changes i.e., their transcriptomic reaction norms. By characterizing the networks of coexpressed genes in each species and their responses to standardized environmental stimuli, we could compare the transcriptomic sensitivity to environmental conditions in the different lineages (Casasa et al., 2020), and identify modules within networks of orthologous genes associated with differences in plasticity across lineages.

Ancestral plasticity in developmental rate in spadefoot toad larvae has evolved into genetically accommodated differences among species in their developmental sensitivity to pond drying (Gomez-Mestre & Buchholz, 2006; Kulkarni et al., 2017). Pelobatoid frogs encompass the largest differences in developmental rate within anuran amphibians. At the two ends of this spectrum are the Western spadefoot toad (*Pelobates cultripes*) and Couch's spadefoot toad (*Scaphiopus couchii*). In benign conditions of high-water levels and food abundance, *P. cultripes* larvae develop slowly and attain large sizes at metamorphosis, although they are capable of accelerating their development upon detection of a reduction in water level, shortening their larval period by as much as 40%. This environmental sensitivity is controlled by the hypothalamic-pituitary-thyroid (HPT) and the hypothalamic-pituitary-inter-renal (HPI) axes (Denver et al., 2002), which regulate developmental acceleration by increasing thyroid hormone and corticosterone levels, expression of thyroid hormone receptors and metabolic rate (Gomez-Mestre et al., 2013; Kulkarni et al., 2017). However, developmental acceleration comes at the expense of reduced size at metamorphosis, consumption of their fat bodies and increased oxidative stress (Gomez-Mestre et al., 2013; Kulkarni et al., 2011, 2017). In comparison, *S. couchii* tadpoles have greatly reduced the ancestral plasticity and have evolved an overall faster developmental rate (the fastest known in anurans; Buchholz & Hayes, 2002), and accordingly, show a constitutively higher metabolic rate and base levels of thyroid hormone and corticosterone compared to *P. cultripes* (Kulkarni et al., 2017). Still unclear however, is how these accommodated changes in developmental plasticity across species are reflected at the transcriptomic level.

Under the null hypothesis that tadpoles of both species show at least some sensitivity to ponds drying out, a reduction in water level will trigger the HPT and HPI axes to accelerate development. Gene

expression in *S. couchii* is expected to experience greater differences over the same absolute time because development proceeds at a faster pace than in *P. cultripes*. Alternatively, because greater plasticity is expected to be the result of greater differential gene expression (e.g., Casasa et al., 2020), we also hypothesize that *P. cultripes*, with its significantly greater developmental plasticity, will experience accordingly greater changes in differential gene expression between normally developing and induced, fast developing tadpoles. Taking advantage of recently published de novo transcriptomes of *P. cultripes* and *S. couchii* (Liedtke et al., 2019), we test these hypotheses by performing RNA-Seq experiments in which we exposed tadpoles of both species to simulated pond drying at the same developmental stage and compare their gene expression profiles over multiple time points to control tadpoles reared in constant water levels.

2 | MATERIALS AND METHODS

2.1 | Experimental design and transcriptome assembly

Sample collection, transcriptome sequencing and de novo assembly are detailed in Liedtke et al. (2019) and published as part of the NCBI BioProject PRJNA490256. In brief, we individually raised tadpoles from single clutches (i.e., siblings) of *P. cultripes* and *S. couchii* in 3 L aquaria (water column = 18.5 cm) under laboratory conditions until they reached a stage at which developmental responses to water level reduction are maximum in these species (Gosner stage 35; Gosner, 1960; Kulkarni et al., 2011). At this point, we dropped the water level of half the tadpoles from each species to 675 ml (4 cm) to trigger developmental acceleration. We very briefly removed tadpoles from their containers to extract the water, also manipulating in the same way tadpoles remaining in the constant water treatment. After that, tadpoles in the constant water treatment of both species were maintained for 24 h. We maintained *P. cultripes* tadpoles in reduced water for a period of 24, 48 or 72 h, and *S. couchii* tadpoles for 24 or 48 h. *Scaphiopus couchii* develops so quickly that we did not include a 72 h time point in our RNA-Seq analysis because development may have progressed within that timeframe. Within the timeframe used, however, we did not observe advancement in developmental stage for either species, and the comparison was therefore stage-matched (at Gonser 35). This experimental procedure follows Gomez-Mestre et al. (2013) and elicits accelerated development in these species, even if the response of *S. couchii* is much less pronounced than that of *P. cultripes* (Kulkarni et al., 2011, 2017). At the end of each time period, and after 24 h for the controls, we euthanized three tadpoles per species, eviscerated and homogenized them for total RNA extraction. We extracted RNA using a Trizol extraction method following the manufacturer's protocol (Invitrogen), and sequenced 21 TruSeq libraries using a HiSeq2000 (Illumina) sequencer in paired end mode with the read length 2 × 76 bp, generating on average 38 million paired-end reads per library. We assembled de novo transcriptomes for both species, based on 12 libraries for each species,

using the Trinity pipeline (Haas et al., 2013), annotating them with Trinotate (<https://trinotate.github.io/>).

2.2 | Transcript abundance and differential gene expression

A schematic representation of the bioinformatic workflow and analytical procedures followed in this study is shown in Supporting Information 1. We estimated transcript abundance using KALLISTO v04.3.1 (Bray et al., 2016) at the Trinity “gene” level and we explored clustering of individuals by treatment using a principal component analysis on the standardized counts (log 2 counts per million). We used EDGER v3.26.6 (McCarthy et al., 2012) to identify differentially expressed transcripts for across all possible combinations of pairwise comparisons of treatment group per species (a total of six comparisons for *P. cultripes* and three for *S. couchii*). Each group consisted of three biological replicates, and we deemed genes with a false discovery rate of $q < 0.05$ and absolute log fold change > 2 as significantly differentially expressed.

To identify genes that show correlated expression patterns over time, we singled out genes that were differentially expressed for at least one pairwise comparison and performed a clustering analysis on their standardized expression values across all treatments. We normalised the count data for these genes using the trimmed mean of M-values (TMM) method in EDGER and averaged across replicates to obtain mean expression per treatment. Subsequently, we standardized expression values per treatment to have mean = 0, SD = 1 and clustered using the soft clustering in MFUZZ v2.44.0 (Kumar & Futschik, 2007). We set the fuzzification parameter to 1.8 and determined the number of clusters by graphically exploring the minimum centroid distance between a range of cluster numbers, choosing as cutoff the number of clusters above which this distance was no longer substantially reduced. We then assigned genes to clusters based on their maximum membership probability.

We performed functional enrichment analyses using g:Profiler (R package GPROFILER2 v0.1.5; Raudvere et al., 2019) on differentially expressed genes at each time point compared to the high water control. For this enrichment analysis, we used transcriptome annotations based on the *Xenopus tropicalis* proteome as the background domain and differentially expressed genes per pairwise comparison as the query (see Liedtke et al., 2019). We used the gSCS correction algorithm of g:Profiler to correct for multiple testing and included the following ontologies and pathway databases: GO-Biological Processes, GO-Cellular Component, GO-Molecular Function, KEGG and REACTOME databases (versions e94_eg41_p11).

2.3 | Coexpression analysis – orthologue assignment

We identified orthologues between *P. cultripes* and *S. couchii* using the HaMStR pipeline (Ebersberger et al., 2009). HaMStR compares query sequences (based on open reading frames: ORFs) with reference proteins

from curated databases and profile hidden Markov models (pHMMs) derived from alignments of reference proteins. Orthologues are identified when there is reciprocity between query sequence, reference protein and pHMM. We downloaded our reference proteins from ORTHO DB v.9 (Kriventseva et al., 2007 accessed 28/03/2018). As only one amphibian species was available from ORTHO DB (the western clawed frog, *X. tropicalis*), we completed our reference protein database with two reptile species (the Chinese softshell turtle *Pelodiscus sinensis* and the American Alligator *Alligator mississippiensis*) and the West Indian Ocean coelacanth *Latimeria chalumnae*. We aligned reference protein sequences using PRANK v.170427 (Löytynoja, 2014), and created the pHMMs using HMMER v.3.1b2 (Zhang & Wood, 2003). HaMStR uses hmmsearch to match query sequences with pHMMs and then BLASTP to compare query sequences to the original reference proteins from *X. tropicalis*. Query sequences for which the top scoring *X. tropicalis* BLASTP hit also contributed to the pHMM hit passed the reciprocity test and were added to a list of target species orthologues.

When multiple orthologues matched a single ORF, we removed the hits based on: (i) the taxonomic specificity of the reference protein (tetrapod proteins took precedence over metazoan proteins); (ii) whether the ORF was the most representative hit (if an ORF was the best hit for one orthologue, but not for one or more other orthologues, we removed it in these other cases); and (iii) E-values, in cases where an ORF was the best hit for more than one orthologue, or in cases where it was never the best hit.

2.4 | Coexpression analysis – network analysis

We normalised transcript count data (Trinity “isoform” level) for each species separately using the trimmed mean of M-values (TMM) method in EDGER and extracted counts per million (cpm) values. When a transcript contained more than one ORF for which there was a matching orthologue, we divided cpm values by the number of ORFs contained within that transcript. We then matched these adjusted cpm values to their respective orthologue. In many cases an orthologue was represented by multiple isoforms. In these cases, we averaged cpm values across isoforms to determine a single representative orthologue count value. We then combined results for both species and only took forward for network analysis orthologues that were present in both species.

We performed a weighted gene correlation network analysis (WGCNA; Langfelder & Horvath, 2008) for the combined data set containing count values for all 21 libraries. Such combination of transcriptomes from multiple species in network analyses can highlight evolutionarily shared and divergent patterns of gene expression (Morandin et al., 2016). We checked data to ensure that orthologues did not contain too many missing values, and assessed the scale-free topology to select an appropriate soft thresholding power by which to raise pairwise correlations of expression. We transformed orthologue coexpression similarity into a signed adjacency matrix based on the selected soft threshold power, and hierarchical clustering identified modules of highly interconnected genes (with a minimum module size of 30). We merged highly similar modules, i.e., those for which module eigengenes

were highly correlated (cutoff set at 0.2). The eigengene is defined as the first principal component of a module and provides a single representative profile of orthologue expression for a given module.

2.5 | Relation of coexpression modules to experimental factors

We assessed the relationships between coexpression modules and species, developmental time and water level treatment by fitting linear models with eigengene values for each module as the response variable. We considered species and water level as factors, and we included time (24 and 48 h only) as a covariate. We assessed the effects of the factors and covariate using the ANOVA function from the car package in R (Fox & Weisberg, 2011). We also initially included the interaction terms species:time, and species:water, but removed them when not significant ($p > .05$), refitting the model.

2.6 | Coexpression analysis – enrichment analysis and visualization

We carried out functional enrichment analysis of gene ontology terms, KEGG and Reactome gene pathways for modules of interest, i.e., those significantly associated with species, water level, time or one of the interactions. We carried out the enrichment analysis in the R package GPROFILER2, using as background domain the previously identified orthologues from the *X. tropicalis* proteome.

To further explore the orthologues involved in response to water level treatment, we calculated gene significance (GS) values in WGCNA (defined as the absolute value of the correlation between orthologue and a given variable, factor or trait; Langfelder & Horvath, 2008). For all modules, we extracted orthologues with a GS p -value ($p.GS$) $<.05$ and visualised them using CYTOSCAPE v 3.8.0 (Shannon et al., 2003), with nodes (orthologues) linked by edges (expression correlations) determined by WGCNA. We only visualised edges with edge values >0.025 , removing nodes without edges.

3 | RESULTS

3.1 | Transcript abundance and differential gene expression

The principal component analysis on the standardized count data (counts per million) for *P. cultripes* samples resulted in overlapping clusters of treatment groups on the first two axes, together

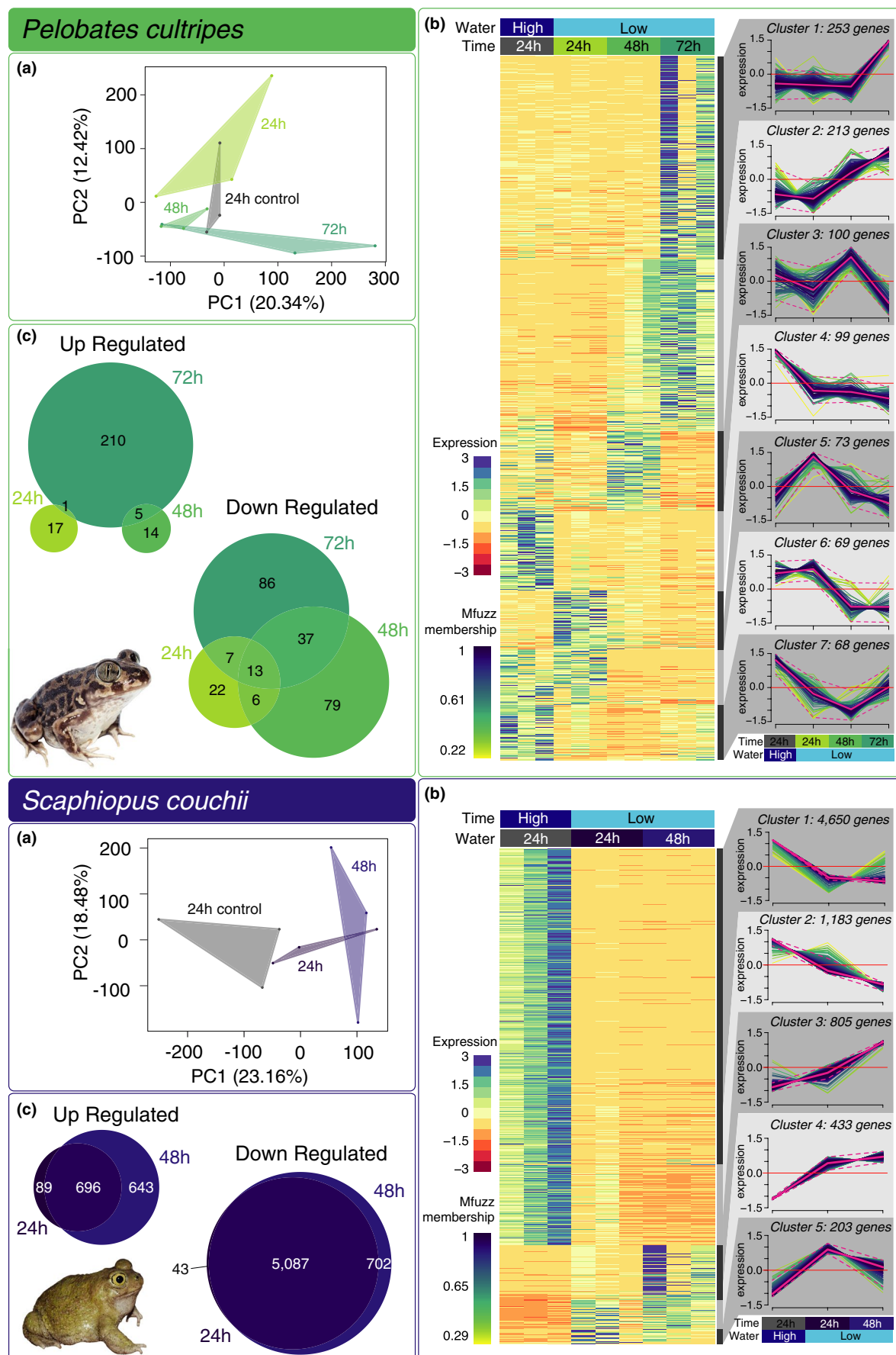
explaining 32.76% of the variance (Figure 1a). Out of a total of 428,406 Trinity “genes”, 875 were differentially expressed in at least one pairwise treatment comparison (0.20%), which MFUZZ soft clustering grouped into seven distinct expression profiles (Figure 1b). The majority of genes (446 genes; clusters 1 and 2) were upregulated after 48 or 72 h of exposure to low water levels, whereas 236 genes (clusters 4, 6 and 7) were downregulated either after 24 or 48 h of exposure. The remaining two clusters (3 and 5; 173 genes) are characterized by time point specific upregulation at 48 and 24 h.

For *S. couchii*, the PCA clustered biological replicates into treatments mostly along PC1 (Figure 1a), which explained 23.16% of the variance in gene counts. 7274 Trinity “genes” out of a total of 381,135 (1.91%) were significantly differentially expressed in at least one pairwise comparison, with MFUZZ optimally fitting these genes into five clusters (Figure 1b). The vast majority of these genes (5833 genes; clusters 1 and 2) were downregulated after 24 or 48 h of exposure to low water, with the remaining genes experiencing upregulation after either 24 (636 genes; clusters 4 and 5) or 48 h (805 genes; cluster 3).

When comparing differentially expressed genes at each time point with the 24 h high water control (Figure 1c), *P. cultripes* exhibited 18 upregulated genes and 48 downregulated genes in the first 24 h of exposure to low water levels, compared to 785 upregulated and 5130 downregulated genes in *S. couchii* (Figure 1c). After 48 h of exposure, 19 genes were upregulated versus 135 downregulated genes in *P. cultripes*, compared to 1339 genes upregulated and 5789 downregulated genes in *S. couchii*. After 72 h of exposure, *P. cultripes* exhibited the most differential expression with an upregulation of 216 genes and a downregulation of 143 genes. Intersections of consistently up- or downregulated genes across time points were relatively small for *P. cultripes* suggesting that the tadpoles were undergoing distinct expression changes per time point, whereas this was not the case for *S. couchii*, with largely overlapping expression profiles at both 24 and 48 h of exposure to low water. Raw counts and all EDGER differential gene expression results are provided as Supporting Information 2 and 3.

When comparing enriched functional terms within species (Figure 2; Supporting Information 4), *P. cultripes* showed no overlap for those enriched at 24 h versus the other two time points, but nine functionally enriched terms were shared by the 48 and 72 h time points (12.68% and 10.98% respectively). In *S. couchii*, overlap in functional terms was substantially greater with 638 of the same terms being enriched at 24 and 48 h (95.51% and 90.50% respectively). When comparing enriched functional terms detected in both species, 67 enriched terms were shared. The number of shared terms increased with time, with the greatest overlap occurring between 72 h in *P. cultripes* and 24 and 48 h in *S. couchii* (47 and 48 terms, respectively). *Pelobates*

FIGURE 1 (a) Principal component biplots of scaled and centred log₂ transcript counts per million and (b) Heatmap visualization of normalized log₂ TMM matrix reduced to only genes that were significantly differentially expressed for at least one pairwise comparison of treatments and clustered based on MFUZZ soft clustering. Heatmap colours show mean-centred normalized expression values. MFUZZ plots show standardized expression of genes per MFUZZ cluster where the colour of each gene's reaction norm reflects the cluster maximum membership probability. Deep pink lines showing the cluster centroids (full lines) and 95% cutoff for gene membership (dashed lines). (c) Euler plots of numbers of up- and downregulated genes for pairwise comparisons of each time point with the high water control



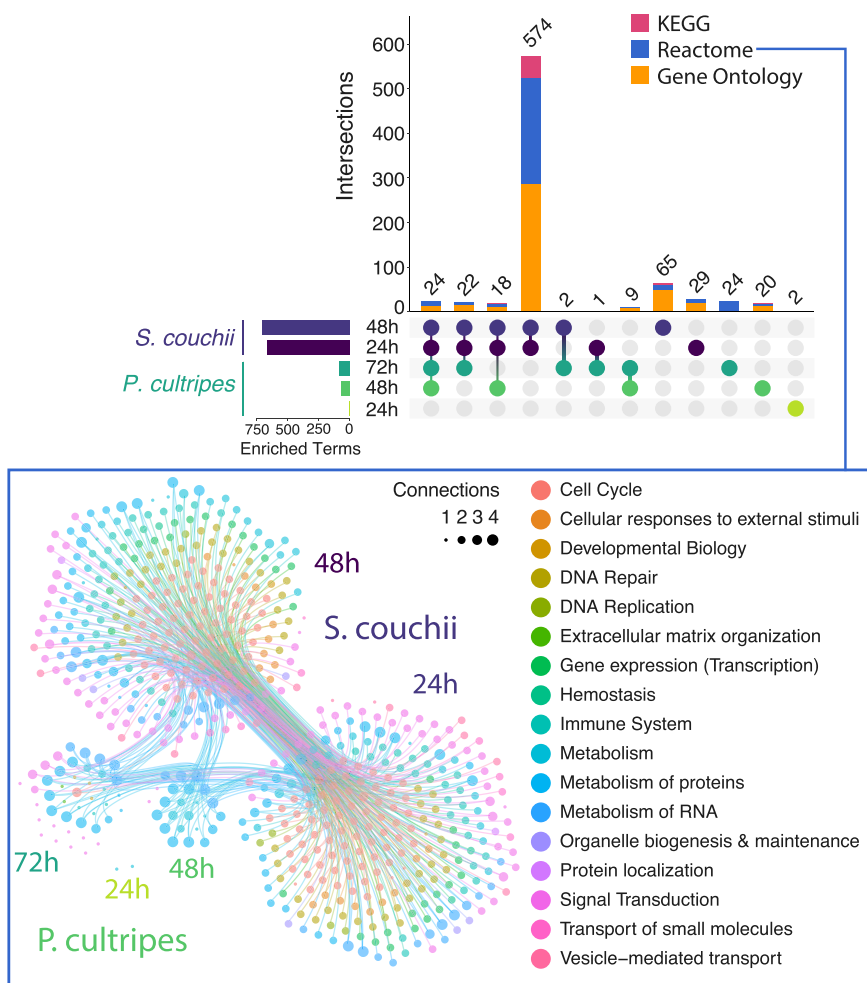


FIGURE 2 Upset diagram showing the number of unique and shared enriched functional terms across time points per species. Vertical bars show the number of intersecting terms (KEGG, Reactome and Gene Ontology shown in distinct colours) for relationships indicated by the connections on the switchboard below. Horizontal bars show total number of enriched terms per time point per species. Insert (blue box) shows the relationships of all Reactome pathways across time points and species, each represented as dot clusters. Each dot represents a Reactome pathway. The same pathways found in multiple clusters are connected by edges and the dot size reflects the number of connections. Pathways (dots) and connections (edges) are colour coded based on the root levels of annotation in the Reactome hierarchy

cultripes was therefore experiencing a delay of up to 48 h in changes in activity of some pathways and processes whose response to pond drying is conserved across the two species. Among these is apoptosis (KEGG:04210; Supporting Information 4), an important process in amphibian metamorphosis (Ishizuya-Oka et al., 2010; Kerr et al., 1974).

At 48 and 72 h of exposure to low water levels, *P. cultripes* saw expression changes in terms related to sterol biosynthesis (GO:0016126), cholesterol biosynthesis (REAC:R-XTR-191273), sterol metabolic processes (GO:0016125) and lipid biosynthetic process (GO:0008610), which were not present in the *S. couchii* enrichment sets. At 72 h, specifically, nine enriched terms related to ribosomal processes were recovered for *P. cultripes* suggesting extensive transcriptional activity. Terms related to HSP90 chaperone cycle for steroid hormone receptors (REAC:R-XTR-3371497) and regulation of thyroid hormone activity (REAC:R-XTR-350864) were also identified at this time point, but were not significantly enriched ($q > 0.05$). The large numbers of significantly enriched Reactome pathways found only in *S. couchii* were mostly related to cell cycle, cellular response to external stimulus, DNA repair and DNA replication (warmer colours in Figure 2 insert), such as signalling by Hedgehog (REAC:R-XTR-5358351), signalling by WNT (REAC:R-XTR-195721) and telomere maintenance (REAC:R-XTR-157579), suggesting that tadpoles of this species are probably experiencing greater cell replication and developmental

advancements in the same or less time than *P. cultripes*. In contrast, Reactome pathways that were uniquely enriched in *P. cultripes* were related to metabolism of proteins and signal transduction (cooler colours in Figure 2 insert).

3.2 | Coexpression analysis – orthologue assignment

Orthology detection based on the 31,745 *X. tropicalis* protein sequences in ORTHO DB identified a total of 12,876 orthologues (Supporting Information 5): 12,386 were present in the *P. cultripes* transcriptome, corresponding to 76,685 isoforms (15,555 unigenes); whereas 12,429 were present in the *S. couchii* transcriptome, corresponding to 94,853 isoforms (from 13,807 unigenes). Of the 12,876 orthologues, 11,939 were present in both target species. Only these shared orthologues were taken forward for network analysis.

3.3 | Coexpression analysis – network analysis

A soft thresholding power of 20 was chosen for the network analysis, corresponding to a scale-free topology model fit R^2 value

of 0.9, at a point where R^2 values began to asymptote. The scale free topology and mean connectivity for different soft threshold powers are shown in Supporting Information 6. Initial hierarchical clustering of orthologues identified 16 coexpression modules, which were reduced to eight following merging of similar modules which then contained between 38 and 7731 orthologues, leaving a “grey” unclustered orthologues module (Table 1; Supporting Information 6).

Module eigengenes were significantly associated with one or more explanatory variables or interactions for five of the eight modules (Table 1; Figure 3). The “blue”, “green”, “turquoise” and “greenyellow” modules were the four largest modules (together

containing 11,368 out of 11,939 orthologues), and each of these was highly significantly associated with species (see Table 1 for F values and p -values). The “blue” (2700 orthologues) and “green” (473 orthologues) modules showed higher expression in *P. cultripes* than *S. couchii* (Figure 3b,c), while the “turquoise” (7731 orthologues) and “greenyellow” (464 orthologues) modules showed higher expression in *S. couchii* relative to *P. cultripes* (Figure 3d,e). The “cyan” module was relatively small (58 orthologues), but showed significant species-by-water interaction ($F = 8.15$, $p = .014$; Table 1): *P. cultripes* exhibited a steep decrease in eigengene expression in response to water drop, while *S. couchii* eigengene expression did not respond to water level (Figure 3a).

TABLE 1 Relationship between seven co-expressed module eigengenes and the experimental variables of species, water and time (24 and 48 h of exposure). Species:water and species:time interactions were initially considered but were dropped when statistically nonsignificant. Significant terms ($p < .05$) are highlighted in bold. The grey module represents unclustered orthologues and was therefore not included in statistical tests

Module	Orthologues	Variable	Sum of squares	df	F value	p-value
Cyan	54	Species	0.0013	1	0.0407	.8432
		Water	0.1564	1	4.7598	.0481
		Time	0.0089	1	0.2704	.6118
		Species:water	0.2678	1	8.1497	.0135
		Residuals	0.4272	13		
Blue	2700	Species	0.7364	1	401.846	<.0001
		Water	0.0001	1	0.068	.7981
		Time	0.0002	1	0.093	.7649
		Residuals	0.0257	14		
Green	473	Species	0.3768	1	22.0108	<.0001
		Water	0.0018	1	0.1024	.7536
		Time	0.0118	1	0.6865	.4212
		Residuals	0.2397	14		
Turquoise	7731	Species	0.9001	1	681.9803	<.0001
		Water	0.0004	1	0.2741	.6088
		Time	0.0011	1	0.8189	.3808
		Residuals	0.0185	14		
Greenyellow	464	Species	0.2784	1	17.8514	<.0001
		Water	0.0068	1	0.4337	.5208
		Time	<0.0001	1	0.002	.9652
		Residuals	0.2184	14		
Lightcyan	38	Species	0.0009	1	0.4317	.5218
		Water	0.0010	1	0.4746	.5022
		Time	0.0005	1	0.2511	.6241
		Residuals	0.0291	14		
Magenta	160	Species	0.1009	1	2.0552	.1736
		Water	0.0198	1	0.4033	.5356
		Time	0.0362	1	0.7371	.4050
		Residuals	0.6875	14		
Black	260	Species	0.0047	1	1.3895	.2581
		Water	0.0008	1	0.2252	.6424
		Time	0.0002	1	0.0543	.8190
		Residuals	0.0469	14		
Grey	59					

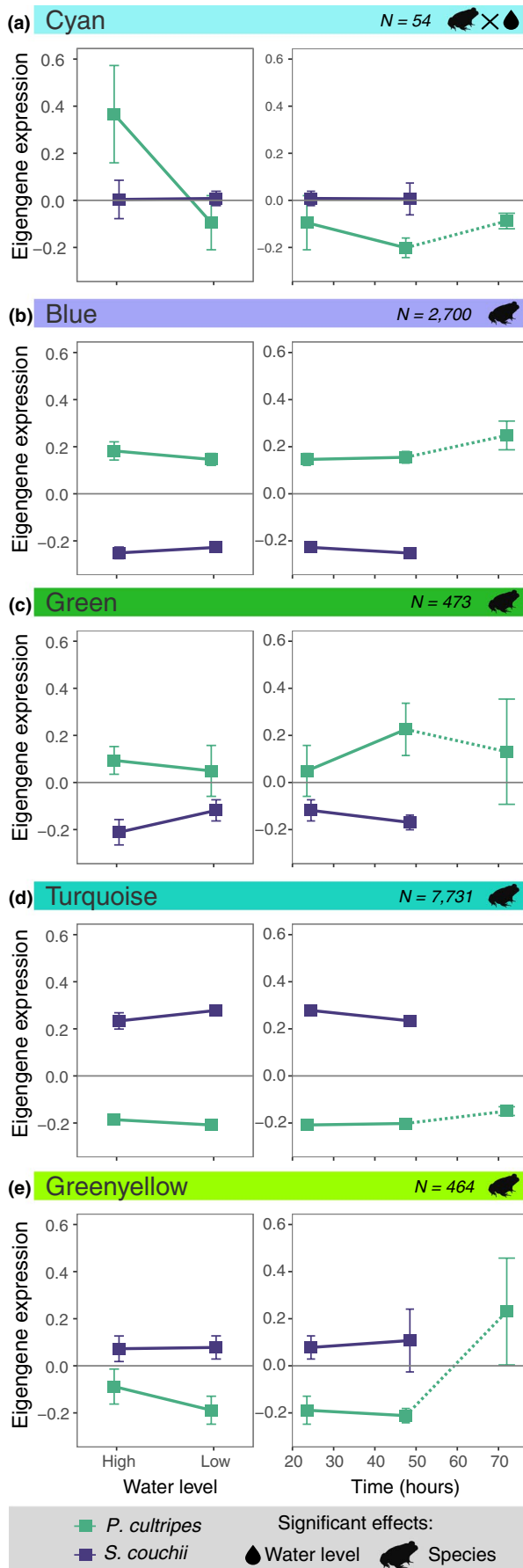


FIGURE 3 Comparison of *P. cultripes* and *S. couchii* eigengene expression for five modules (a–e) in which either species as a main effect or the species:water interaction was a significant factor (as indicated). Error bars denote standard error and the number of orthologues per module are indicated. For each module, two plots are presented, showing eigengene expression under different water treatments at 24 h (left hand plots), and in low water conditions over the course of the experiment (right hand plots). Eigengene expression for *P. cultripes* at 72 h is shown (connected by a dashed line), but was not included in statistical analyses when determining the factors that influenced eigengene expression

None of the modules identified had a significant shared plastic response to reduced water level (i.e., water effect with no significant species interaction), nor did we observe a significant time effect in any module. Taken with the strong species effects observed for the four largest modules, these results suggest few unifying patterns of coexpression in response to reduced water level and over time between the species. Yet despite the overwhelming divergent baseline signals in eigengene expression, the analysis was able to identify a module of 54 orthologues with environmental sensitivity to reduced water levels in *P. cultripes* that was not environmentally sensitive in *S. couchii*.

3.4 | Coexpression analysis – functional enrichment analysis and network visualisation

A full list of significantly enriched functions for all modules can be found in Supporting Information 5, and a summary of top terms (up to the five most significant for the three main GO domains of biological process, molecular function and cellular component, and KEGG and Reactome pathways) is provided in Table 2. Here, we briefly describe some of the main functionally enriched pathways from the *Xenopus* Reactome. For the “cyan” module, associated with species differences in developmental plasticity to decreased water level, the five most significantly enriched Reactome pathways (Table 2; Supporting Information 7) were associated with general metabolism (REAC:R-XTR-1430728) lipid and steroid metabolism (R-XTR-556833 and R-XTR-8957322), cholesterol biosynthesis (R-XTR-191273) and cysteine formation from homocysteine (REAC:R-XTR-1614603). The “green” module, which showed higher eigengene expression in *P. cultripes* than *S. couchii* was associated with immune system and complement pathways (REAC:R-XTR-168256, REAC:R-XTR-166658 and REAC:R-XTR-166663), while the “greenyellow” module, which showed higher expression in *S. couchii* than *P. cultripes*, was associated with the cell cycle and mitosis (R-XTR-69278, R-XTR-1640170, REAC:R-XTR-68882, R-XTR-68886, and R-XTR-2555396). The “blue” and “turquoise” modules were not functionally enriched for any Reactome pathways, probably due to their large sizes and un-specialised natures, although various GO biological processes and cellular components associated with muscular development were enriched in the “blue” module (higher eigengene expression in *P. cultripes*) and the GO molecular function “transferase activity” was

TABLE 2 Summary of top five significantly enriched GO:BP, GO:MF, GO:CC, KEGG and REAC terms for each of the five modules significantly associated with one of the experimental variables (main effects of species, water, time, and interactions of species:water or species:time)

Module	Term ID	Source	Term name	p-value	Associations
Cyan	GO:0044281	GO:BP	Small molecule metabolic process	1.31E-06	species:water
	GO:0006082	GO:BP	Organic acid metabolic process	4.71E-06	
	GO:0019752	GO:BP	Carboxylic acid metabolic process	2.86E-05	
	GO:0043436	GO:BP	Oxoacid metabolic process	4.36E-05	
	GO:0006418	GO:BP	tRNA aminoacylation for protein translation	1.36E-03	
	GO:0017101	GO:CC	Aminoacyl-tRNA synthetase multienzyme complex	9.79E-03	
	GO:0016875	GO:MF	Ligase activity, forming carbon-oxygen bonds	4.11E-04	
	GO:0004812	GO:MF	Aminoacyl-tRNA ligase activity	4.11E-04	
	GO:0048037	GO:MF	Cofactor binding	1.20E-03	
	GO:0003824	GO:MF	Catalytic activity	1.15E-02	
	GO:0140101	GO:MF	Catalytic activity, acting on a tRNA	1.17E-02	
	KEGG:00970	KEGG	Aminoacyl-tRNA biosynthesis	2.77E-08	
	KEGG:00100	KEGG	Steroid biosynthesis	4.16E-05	
	KEGG:01100	KEGG	Metabolic pathways	5.12E-03	
	KEGG:00860	KEGG	Porphyrin and chlorophyll metabolism	1.36E-02	
	REAC:R-XTR-191273	REAC	Cholesterol biosynthesis	3.00E-06	
	REAC:R-XTR-1430728	REAC	Metabolism	2.27E-04	
	REAC:R-XTR-556833	REAC	Metabolism of lipids	2.30E-03	
	REAC:R-XTR-1614603	REAC	Cysteine formation from homocysteine	5.03E-03	
	REAC:R-XTR-8957322	REAC	Metabolism of steroids	1.09E-02	
Blue	GO:0061061	GO:BP	Muscle structure development	6.93E-03	species
	GO:0060537	GO:BP	Muscle tissue development	4.66E-02	
	GO:0014706	GO:BP	Striated muscle tissue development	4.66E-02	
	GO:0030017	GO:CC	Sarcomere	7.98E-06	
	GO:0030016	GO:CC	Myofibril	1.68E-05	
	GO:0043292	GO:CC	Contractile fibre	3.40E-05	
	GO:0044449	GO:CC	Contractile fibre part	3.40E-05	
	GO:0031674	GO:CC	I band	1.29E-03	
	KEGG:00190	KEGG	Oxidative phosphorylation	3.47E-02	

(Continues)

TABLE 2 (Continued)

Module	Term ID	Source	Term name	p-value	Associations
Green	GO:0030479	GO:CC	Actin cortical patch	.01621694	species
	GO:0061645	GO:CC	Endocytic patch	.01621694	
	REAC:R-XTR-168256	REAC	Immune system	.001388036	
	REAC:R-XTR-166658	REAC	Complement cascade	.001677751	
	REAC:R-XTR-166663	REAC	Initial triggering of complement	.004812868	
Turquoise	GO:0016740	GO:MF	Transferase activity	.02786509	species
Greenyellow	GO:0007049	GO:BP	Cell cycle	1.19E-10	species
	GO:0022402	GO:BP	Cell cycle process	1.47E-08	
	GO:0000278	GO:BP	Mitotic cell cycle	2.30E-08	
	GO:0006260	GO:BP	DNA replication	2.71E-08	
	GO:1903047	GO:BP	Mitotic cell cycle process	5.28E-07	
	GO:0005694	GO:CC	Chromosome	2.20E-10	
	GO:0044427	GO:CC	Chromosomal part	5.74E-09	
	GO:0000793	GO:CC	Condensed chromosome	3.34E-07	
	GO:0000779	GO:CC	Condensed chromosome, centromeric region	2.58E-06	
	GO:0000502	GO:CC	Proteasome complex	2.62E-05	
	GO:0042393	GO:MF	Histone binding	1.68E-02	
	KEGG:03030	KEGG	DNA replication	5.09E-08	
	KEGG:04110	KEGG	Cell cycle	7.56E-05	
	KEGG:04114	KEGG	Oocyte meiosis	4.04E-03	
	KEGG:03050	KEGG	Proteasome	3.66E-02	
	REAC:R-XTR-1640170	REAC	Cell cycle	3.82E-30	
	REAC:R-XTR-69278	REAC	Cell cycle, mitotic	2.51E-29	
	REAC:R-XTR-68882	REAC	Mitotic anaphase	1.19E-18	
	REAC:R-XTR-2555396	REAC	Mitotic metaphase and anaphase	1.59E-18	
	REAC:R-XTR-68886	REAC	M phase	4.26E-18	

enriched in the “turquoise” module (higher eigengene expression in *S. couchii*).

Across all modules, 149 orthologues were found to have a significant ($p_{GS} < .05$) association with water (Supporting Information 8). The network visualization (Figure 4) shows 52 of these water-associated orthologues which had at least one interaction (adjacency >0.025) with another water-associated orthologue. Orthologues from the “cyan” and “turquoise” modules showed greater numbers of intramodule connections. The strongest pattern of coexpression (many adjacency values >0.1) was observed in six orthologues in the “cyan” module: mevalonate kinase, mevalonate (diphospho) decarboxylase, NAD(P) dependent steroid dehydrogenase-like, phosphatidylserine synthase 2 and cystathionine gamma-lyase. All six of these orthologues contributed to at least one of the significantly enriched Reactome pathways (general, lipid, and steroid metabolism, cholesterol biosynthesis and cysteine formation from homocysteine).

The orthologues with the strongest associations with water are not necessarily shown in the network due to low adjacency values with other nodes, although stomatin (EPB72)-like 2 and TP53 regulating kinase from the “cyan” module, and uroporphyrinogen III synthase and pancreas specific transcription factor 1a (PTF1) from the “turquoise” module were among the top 10 most significant ($p < .004$) and are included in Figure 4.

4 | DISCUSSION

Transcriptomic approaches permit a more comprehensive screening for environmentally sensitive gene regulatory networks than candidate gene approaches, and are thus advantageous for studying complex evolutionary processes such as developmental plasticity and genetic accommodation (Aubin-Horth & Renn, 2009;

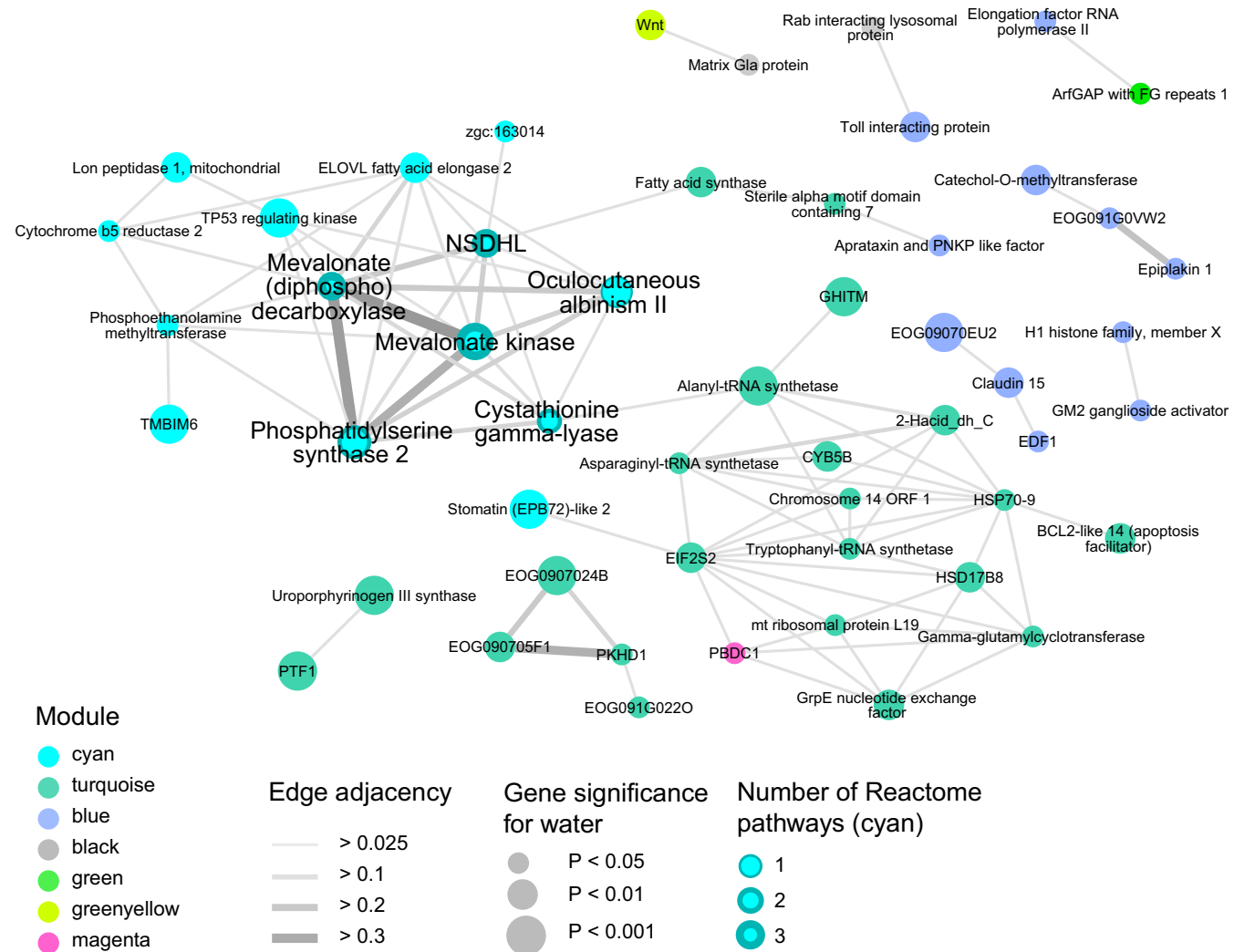


FIGURE 4 Network of coexpressed orthologues with significant water effects ($p_{GS} < .05$) across all modules. Nodes are coloured based on module of origin (see Figure 3). Edges with adjacency values <0.025 are not included, and nodes without at least one edge were excluded. Edge thickness corresponds to adjacency value and node size corresponds to gene significance for water (the largest nodes having p_{GS} values $< .001$). Those orthologues in the water-sensitive cyan module which contributed towards enriched Reactome functions are highlighted with node borders (thicker borders indicating contribution to more functions) and enlarged labels. The Reactome functions and full names of abbreviated orthologues can be found in Supporting Information 8

Beldade et al., 2011; Sommer, 2020; Young, 2013). The prevailing signal in the transcriptomic data was attributable to species differences, regardless of experimental manipulation of water level. This is not surprising given more than 120 million years of independent evolution between these species and considerable divergences of their genomes (Liedtke et al., 2018; Zeng et al., 2014). As has been shown for other systems (e.g., Casasa et al., 2020), we initially hypothesized that *P. cultripes* would manifest greater regulatory response to a reduction in water level than *S. couchii*, due to its more pronounced developmental plasticity. However, the developmentally more canalized *S. couchii* showed around eight times the number of differentially expressed genes in response to reduced water level compared to *P. cultripes*. The development of *S. couchii* is also known to be responsive to pond drying (Kulkarni et al., 2011; Newman, 1989), but this result is nonetheless unexpected, given that in comparison to *P. cultripes*, its developmental rate is very robust to external perturbations including variation in water level, the addition of exogenous corticosterone, or the inhibition of corticosterone synthesis (Kulkarni et al., 2017). However, physiological systems consist of complex networks that arise from interacting units and feedback loops (Burggren & Monticino, 2005; Sturmberg et al., 2015) and physiological processes in organisms in their prime state are tightly regulated so that every small deviation is immediately corrected (Goldberger et al., 2002; Vargas et al., 2015). Maintaining the course of development in *S. couchii* in the face of environmental fluctuations may require a buffering mechanism that constantly adjusts the underlying developmental and physiological processes, thus also causing frequent adjustments in gene expression.

The developmental and metabolic rates of *S. couchii* tadpoles in benign conditions are substantially higher than those of *P. cultripes*, and thus, the observed results also fit our null hypothesis; only slight acceleration (i.e., lower plasticity) of an already accelerated system (*S. couchii*) may be enough to result in greater gene expression change in very short periods of time. This is supported by the network analysis which shows that the majority of orthologues are assigned to modules with consistently higher expression levels in *S. couchii* regardless of water level (the *S. couchii* associated modules "turquoise" and "greenyellow" contained more than 2.5 times as many orthologues as the *P. cultripes* associated modules of "blue" and "green"). These highly expressed orthologues make up pathways related to cell cycle, mitosis and DNA replication, possibly reflecting the faster absolute development in this species. In addition, *P. cultripes* shows a lagged or slower response, which may further explain the lower number of differential gene expression in the first 72 h. The single largest MFUZZ cluster in *S. couchii* characterizes expression changes in the first 24 h (cluster 1), but for *P. cultripes*, the biggest response is seen only after 72 h (cluster 1), representing a clear asynchrony in the peaks of expression changes in important processes such as apoptosis. Apoptosis is a major process in amphibian metamorphosis, responsible for the cell death in larval-specific tissue, but also in larval-to-adult remodelling of organs (Ishizuya-Oka et al., 2010; Kerr et al., 1974).

Despite the large differences in the transcriptomic profiles of the two species, the network analysis identified a module of genes whose expression in response to pond drying showed a divergence in transcriptomic reaction norms between species (i.e., a significant species-by-treatment effect). More precisely, genes of this module experienced significant differences in expression in response to pond drying in *P. cultripes*, but not *S. couchii*. We interpret this pattern as a signal of genetic accommodation (Sikkink et al., 2019), because the change in environmental sensitivity of the encompassed genes may be pertinent to the evolutionary differences in developmental plasticity observed between species. The most significant functionally enriched terms in this genetic accommodation module are related to cholesterol and steroid biosynthesis and/or metabolism. Cholesterol biosynthesis is a requisite for synthesis of steroids (LaVoie & King, 2009) including corticosteroids. Environmentally sensitive orthologues involved in cholesterol synthesis, including mevalonate kinase, mevalonate (diphospho) decarboxylase and NSDHL (NAD(P) dependent steroid dehydrogenase-like) showed high levels of coexpression and occupied central positions within the diverged plasticity module. In turn, cystathionine gamma-lyase, which is involved in the metabolism of cholesterol (Mani et al., 2015), showed moderate co-expression with these orthologues and also occupied an important position between the environmentally sensitive "cyan" module and the *S. couchii* associated "turquoise" module. These findings suggest that synthesis and regulation of cholesterol is a key process underlying developmental plasticity in *P. cultripes*, and that its regulation has diverged in *S. couchii*. Differences in pathways associated with lipid metabolism reflect the fact that *P. cultripes* tadpoles experience a >2-fold increase in metabolic rate and deplete their fat reserves during developmental acceleration. In turn, *S. couchii* tadpoles maintain a higher and constant metabolic rate regardless of water level, and produce almost no fat bodies even if metamorphosis is chemically blocked and larvae are fed ad libitum under benign conditions (Kulkarni et al., 2011, 2017). Another two orthologues in the divergent plasticity module which had particularly high gene significance were TP53 regulating kinase and transmembrane Bax inhibitor motif containing 6 (TMBIM6). TP53 is an important regulator of apoptosis (Yogosawa & Yoshida, 2018), whereas Bax is known to induce apoptosis during amphibian metamorphosis (Sachs et al., 2004). Reduced expression of TP53 regulating kinase and the Bax inhibitor TMBIM6 are probably involved in the programmed cell death of larval tissues during accelerated development.

The timing of amphibian larval development is primarily controlled by thyroid hormone acting together with corticosterone (Denver, 1997; Sachs & Buchholz, 2019). Although the role of corticosteroids in accelerating development is less well understood than that of thyroid hormone, it is clear that CORT accelerates thyroid hormone-induced metamorphosis with peak blood levels occurring at the climax of natural metamorphosis (Kulkarni & Buchholz, 2014). Moreover, endogenous CORT levels are known to be facultatively increased in *P. cultripes*, but consistently high in *S. couchii* in the face of pond drying (Kulkarni et al., 2017). In this study, we find that the genes coding for deiodinase 3 (dio3),

an enzyme important for the activation of thyroid hormone and the transcription factor Krüppel-like factor 9 (KLF9), downstream target genes of corticosterone in amphibians (Bonett et al., 2009; Kulkarni & Buchholz, 2014), both experienced a significant positive fold change at 72 h of low water exposure in *P. cultripes*, but were not significantly differentially expressed in *S. couchii*. We interpret this to be confirmatory that genes directly related to the HPI axis were differentially expressed in *P. cultripes* in response to reduced water level, but were not as environmentally sensitive in *S. couchii*.

This first genome-wide scan of the molecular mechanisms of plasticity and canalization of developmental acceleration in two spadefoot toad species is a significant step in our understanding of the evolution of plasticity. Despite the great divergence due to the long period of independent evolution between these species and the fundamentally different rates of development, we could identify a relatively small set of genes that are involved in their divergent responsiveness to the risk of pond drying, i.e., genetic accommodation of developmental plasticity between the species. Future studies must work towards functional verification of the role of the main regulatory genes here identified, and narrow their activity down to the tissue-specific level. Moreover, cross-species divergences in responsiveness to environmental cues is surely reflection of processes also operating within species first, and spadefoot toad populations are likely to have evolved different developmental rates and responsiveness to short hydroperiod, as has been shown for Northern European populations of *Rana temporaria* (Meyer-Lucht et al., 2019; Richter-Boix et al., 2013). Identifying among-population variation in gene regulatory networks regulating plasticity would be key in understanding how the genetically accommodated differences observed across species are initiated.

The role of developmental plasticity in evolution has gained prominence in recent years, but how plasticity itself evolves at the molecular level is only recently being elucidated (Casasa et al., 2020; Levis et al., 2020; Sikkink et al., 2019; Sommer, 2020). By studying two species of spadefoot toad with differing degrees of plasticity in response to pond drying, we identified orthologues and functional gene pathways whose environmental sensitivity in expression (i.e., their transcriptomic reaction norms) have diverged. In doing so, we discerned transcriptomic modules whose evolutionary changes in regulation may be linked to genetic accommodation of developmental plasticity in this system.

ACKNOWLEDGEMENTS

This project was funded by the Ministerio de Economía, Industria y Competitividad (MINECO) through grant CGL2017-83407-P. We also thank D. Buchholz for important and insightful discussions.

AUTHOR CONTRIBUTIONS

Ivan Gomez-Mestre and Hans Christoph Liedtke designed the study and carried out all laboratory work. Hans Christoph Liedtke, Ewan Harney and Ivan Gomez-Mestre conducted analyses and wrote the manuscript.

DATA AVAILABILITY STATEMENT

The raw RNAseq and the transcriptome assemblies have been deposited on the NCBI's Sequence Read Archive (SRP161446) and Transcriptome Shotgun Assembly database (*P. cultripes*: GHBH01000000; *S. couchii*: GHBO01000000), under BioProject PRJNA490256. All processed data sets used in this article are available as Supporting Information (1–8) deposited on dryad (<https://doi.org/10.5061/dryad.cnp5hqc3z>).

ORCID

Ivan Gomez-Mestre  <https://orcid.org/0000-0003-0094-8195>

REFERENCES

- Aubin-Horth, N., & Renn, S. C. P. (2009). Genomic reaction norms: Using integrative biology to understand molecular mechanisms of phenotypic plasticity. *Molecular Ecology*, 18, 3763–3780.
- Beldade, P., Mateus, A. R. A., & Keller, R. A. (2011). Evolution and molecular mechanisms of adaptive developmental plasticity. *Molecular Ecology*, 20, 1347–1363.
- Bonett, R. M., Hu, F., Bagamasbad, P., & Denver, R. J. (2009). Stressor and glucocorticoid-dependent induction of the immediate early gene Krüppel-like factor 9: Implications for neural development and plasticity. *Endocrinology*, 150, 1757–1765.
- Bray, N. L., Pimentel, H., Melsted, P., & Pachter, L. (2016). Near-optimal probabilistic RNA-seq quantification. *Nature Biotechnology*, 34, 525–527.
- Brenner, J. L., Jasiewicz, K. L., Fahley, A. F., Kemp, B. J., & Abbott, A. L. (2010). Loss of individual microRNAs causes mutant phenotypes in sensitized genetic backgrounds in *C. elegans*. *Current Biology*, 20, 1321–1325.
- Buchholz, D. R., & Hayes, T. B. (2002). Evolutionary patterns of diversity in spadefoot toad metamorphosis (Anura: Pelobatidae). *Copeia*, 2002, 180–189.
- Burggren, W. W., & Monticino, M. G. (2005). Assessing physiological complexity. *Journal of Experimental Biology*, 208, 3221–3232.
- Casasa, S., & Moczek, A. P. (2018). The role of ancestral phenotypic plasticity in evolutionary diversification: Population density effects in horned beetles. *Animal Behaviour*, 137, 53–61.
- Casasa, S., Zattara, E. E., & Moczek, A. P. (2020). Nutrition-responsive gene expression and the developmental evolution of insect polyphenism. *Nature Ecology & Evolution*, 4, 1–12.
- Denver, R. J. (1997). Proximate mechanisms of phenotypic plasticity in amphibian metamorphosis. *American Zoologist*, 37, 172–184.
- Denver, R. J., Glennemeier, K. A., & Boorse, G. C. (2002). Endocrinology of complex life cycles: Amphibians. In D. W. Pfaff (Ed.), *Hormones, brain and behavior* (pp. 469–514). Academic Press.
- Draghi, J. A., & Whitlock, M. C. (2012). Phenotypic plasticity facilitates mutational variance, genetic variance, and evolvability along the major axis of environmental variation. *Evolution*, 66, 2891–2902.
- Ebersberger, I., Strauss, S., & von Haeseler, A. (2009). HaMStR: Profile hidden markov model based search for orthologs in ESTs. *BMC Evolutionary Biology*, 9, 157–159.
- Fox, J., & Weisberg, S. (2011). *An R companion to applied regression*. SAGE Publications.
- Frankel, N., Davis, G. K., Vargas, D., Wang, S., Payne, F., & Stern, D. L. (2010). Phenotypic robustness conferred by apparently redundant transcriptional enhancers. *Nature Methods*, 466, 1–5.
- Goldberger, A. L., Peng, C.-K., & Lipsitz, L. A. (2002). What is physiologic complexity and how does it change with aging and disease? *Neurobiology of Aging*, 23, 23–26.
- Gomez-Mestre, I., & Buchholz, D. R. (2006). Developmental plasticity mirrors differences among taxa in spadefoot toads linking plasticity

- and diversity. *Proceedings of the National Academy of Sciences USA*, 103, 19021–19026.
- Gomez-Mestre, I., & Jovani, R. (2013). A heuristic model on the role of plasticity in adaptive evolution: Plasticity increases adaptation, population viability and genetic variation. *Proceedings of the Royal Society B: Biological Sciences*, 280, 20131869.
- Gomez-Mestre, I., Kulkarni, S., & Buchholz, D. R. (2013). Mechanisms and consequences of developmental acceleration in tadpoles responding to pond drying. *PLoS One*, 8, e84266.
- Gosner, K. L. (1960). A simplified table for staging anuran embryos and larvae with notes on identification. *Herpetologica*, 16, 183–190.
- Haas, B. J., Papanicolaou, A., Yassour, M., Grabherr, M., Blood, P. D., Bowden, J., Couger, M. B., Eccles, D., Li, B., Lieber, M., MacManes, M. D., Ott, M., Orvis, J., Pochet, N., Strozzi, F., Weeks, N., Westerman, R., William, T., Dewey, C. N., ... Regev, A. (2013). De novo transcript sequence reconstruction from RNA-seq using the Trinity platform for reference generation and analysis. *Nature Protocols*, 8, 1494–1512.
- Ishizuya-Oka, A., Hasebe, T., & Shi, Y.-B. (2010). Apoptosis in amphibian organs during metamorphosis. *Apoptosis*, 15, 350–364.
- Kerr, J. F. T., Harmon, B., & Searle, J. (1974). An electron-microscope study of cell deletion in the anuran tadpole tail during spontaneous metamorphosis with special reference to apoptosis of striated muscle fibres. *Journal of Cell Science*, 14, 571–585.
- Kriventseva, E. V., Rahman, N., Espinosa, O., & Zdobnov, E. M. (2007). OrthoDB: The hierarchical catalog of eukaryotic orthologs. *Nucleic Acids Research*, 36, D271–D275.
- Kulkarni, S. S., & Buchholz, D. R. (2014). Corticosteroid signaling in frog metamorphosis. *General and Comparative Endocrinology*, 203, 225–231.
- Kulkarni, S. S., Denver, R. J., Gomez-Mestre, I., & Buchholz, D. R. (2017). Genetic accommodation via modified endocrine signalling explains phenotypic divergence among spadefoot toad species. *Nature Communications*, 8, 1–6.
- Kulkarni, S. S., Gomez-Mestre, I., Moskalik, C. L., Storz, B. L., & Buchholz, D. R. (2011). Evolutionary reduction of developmental plasticity in desert spadefoot toads. *Journal of Evolutionary Biology*, 24, 2445–2455.
- Kumar, L., & Futschik, M. E. (2007). Mfuzz: A software package for soft clustering of microarray data. *Bioinformation*, 2, 5–7.
- Lafuente, E., & Beldade, P. (2019). Genomics of developmental plasticity in animals. *Frontiers in Genetics*, 10, 1601–1618.
- Langfelder, P., & Horvath, S. (2008). WGCNA: An R package for weighted correlation network analysis. *BMC Bioinformatics*, 9, 559–613.
- LaVoie, H. A., & King, S. R. (2009). Transcriptional regulation of steroidogenic genes: STARD1, CYP11A1 and HSD3B. *Experimental Biology and Medicine*, 234, 880–907.
- Levis, N. A., Reed, E. M. X., Pfennig, D. W., & Burford Reiskind, M. O. (2020). Identification of candidate loci for adaptive phenotypic plasticity in natural populations of spadefoot toads. *Ecology and Evolution*, 16, 219–313.
- Liedtke, H. C., Gomez Garrido, J., Esteve-Codina, A., Gut, M., Alioto, T., & Gomez-Mestre, I. (2019). De novo assembly and annotation of the larval transcriptome of two spadefoot toads widely divergent in developmental rate. *G3: Genes|Genomes|Genetics*, 9, 2647–2655.
- Liedtke, H. C., Gower, D. J., Wilkinson, M., & Gomez-Mestre, I. (2018). Macroevolutionary shift in the size of amphibian genomes and the role of life history and climate. *Nature Ecology & Evolution*, 2, 1792–1799.
- Londe, S., Monnin, T., Cornette, R., Debat, V., Fisher, B. L., & Molet, M. (2015). Phenotypic plasticity and modularity allow for the production of novel mosaic phenotypes in ants. *EvoDevo*, 6, 1–15.
- Löytynoja, A. (2014). Phylogeny-aware alignment with PRANK. *Methods in Molecular Biology* (Clifton, N.J.), 1079, 155–170.
- Mani, S., Li, H., Yang, G., Wu, L., & Wang, R. (2015). Deficiency of cystathione gamma-lyase and hepatic cholesterol accumulation during mouse fatty liver development. *Science Bulletin*, 60, 336–347.
- McCarthy, D. J., Chen, Y., & Smyth, G. K. (2012). Differential expression analysis of multifactor RNA-Seq experiments with respect to biological variation. *Nucleic Acids Research*, 40, 4288–4297.
- Meyer-Lucht, Y., Luquet, E., Jóhannesdóttir, F., Rödin-Mörch, P., Quintela, M., Richter-Boix, A., Höglund, J., & Laurila, A. (2019). Genetic basis of amphibian larval development along a latitudinal gradient: Gene diversity, selection and links with phenotypic variation in transcription factor C/EBP-1. *Molecular Ecology*, 28(11), 2786–2801.
- Moczek, A. P. (2010). Phenotypic plasticity and diversity in insects. *Philosophical Transactions of the Royal Society B: Biological Sciences*, 365, 593–603.
- Morandin, C., Tin, M. M. Y., Abril, S., Gómez, C., Pontieri, L., Schiøtt, M., Sundström, L., Tsuji, K., Pedersen, J. S., Helanterä, H., & Mikheyev, A. S. (2016). Comparative transcriptomics reveals the conserved building blocks involved in parallel evolution of diverse phenotypic traits in ants. *Genome Biology*, 17, 43.
- Newman, R. A. (1989). Developmental plasticity of *Scaphiopus couchii* tadpoles in an unpredictable environment. *Ecology*, 70, 1775–1787.
- Pigliucci, M., Murren, C. J., & Schlücht, C. D. (2006). Phenotypic plasticity and evolution by genetic assimilation. *Journal of Experimental Biology*, 209, 2362–2367.
- Projecto-Garcia, J., Biddle, J. F., & Ragsdale, E. J. (2019). Decoding the architecture and origins of mechanisms for developmental polyphenism. *Current Opinion in Genetics & Development*, 47, 1–8.
- Raudvere, U., Kolberg, L., Kuzmin, I., Arak, T., Adler, P., Peterson, H., & Vilo, J. (2019). g:Profiler: A web server for functional enrichment analysis and conversions of gene lists (2019 update). *Nucleic Acids Research*, 44, W90–W98.
- Richter-Boix, A., Quintela, M., Kierczak, M., Franch, M., & Laurila, A. (2013). Fine-grained adaptive divergence in an amphibian: Genetic basis of phenotypic divergence and the role of nonrandom gene flow in restricting effective migration among wetlands. *Molecular Ecology*, 22(5), 1322–1340.
- Sachs, L. M., & Buchholz, D. R. (2019). Insufficiency of thyroid hormone in frog metamorphosis and the role of glucocorticoids. *Frontiers in Endocrinology*, 10, 287.
- Sachs, L. M., Le Mevel, S., & Demeneix, B. A. (2004). Implication of baxin *Xenopus laevis* tail regression at metamorphosis. *Developmental Dynamics*, 231, 671–682.
- Schlücht, C. D., & Pigliucci, M. (1998). *Phenotypic evolution: A reaction norm perspective*. Sinauer Associates Incorporated.
- Schlücht, C. D., & Wund, M. A. (2014). Phenotypic plasticity and epigenetic marking: An assessment of evidence for genetic accommodation. *Evolution*, 68, 656–672.
- Schneider, R. F., Li, Y., Meyer, A., & Gunter, H. M. (2014). Regulatory gene networks that shape the development of adaptive phenotypic plasticity in a cichlid fish. *Molecular Ecology*, 23, 4511–4526.
- Schwab, D. B., Casasa, S., & Moczek, A. P. (2019). On the reciprocally causal and constructive nature of developmental plasticity and robustness. *Frontiers in Genetics*, 9, 735.
- Shannon, P., Markiel, A., Ozier, O., Baliga, N. S., Wang, J. T., Ramage, D., Amin, N., Schwikowski, B., & Ideker, T. (2003). Cytoscape: A software environment for integrated models of biomolecular interaction networks. *Genome Research*, 13, 2498–2504.
- Sikkink, K. L., Reynolds, R. M., Ituarte, C. M., Cresko, W. A., & Phillips, P. C. (2019). Environmental and evolutionary drivers of the modular gene regulatory network underlying phenotypic plasticity for stress resistance in the nematode *Caenorhabditis remanei*. *G3: Genes|Genomes|Genetics*, 9, 969–982.
- Snell-Rood, E. C., Van Dyken, J. D., Cruckshank, T., Wade, M. J., & Moczek, A. P. (2009). Toward a population genetic framework of developmental evolution: the costs, limits, and consequences of phenotypic plasticity. *BioEssays*, 32, 71–81.
- Sommer, R. J. (2020). Phenotypic plasticity: From theory and genetics to current and future challenges. *Genetics*, 215, 1–13.

- Sturmberg, J. P., Bennett, J. M., Picard, M., & Seely, A. J. E. (2015). The trajectory of life. Decreasing physiological network complexity through changing fractal patterns. *Frontiers in Physiology*, 6, 283–311.
- Suzuki, Y., & Nijhout, H. F. (2006). Evolution of a polyphenism by genetic accommodation. *Science*, 311, 650–652.
- Vargas, B., Cuesta-Frau, D., Ruiz-Esteban, R., Cirugeda, E., & Varela, M. (2015). What can biosignal entropy tell us about health and disease? Applications in some clinical fields. *Nonlinear Dynamics, Psychology, and Life Sciences*, 19, 419–436.
- West-Eberhard, M. J. (2003). *Developmental plasticity and evolution*. Oxford University Press.
- Yogosawa, S., & Yoshida, K. (2018). Tumor suppressive role for kinases phosphorylating p53 in DNAdamage-induced apoptosis. *Cancer Science*, 109, 3376–3382.
- Young, R. L. (2013). Linking conceptual mechanisms and transcriptomic evidence of plasticity-driven diversification. *Molecular Ecology*, 22, 4363–4365.
- Zeng, C., Gomez-Mestre, I., & Wiens, J. J. (2014). Evolution of rapid development in Spadefoot Toads is unrelated to arid environments. *PLoS One*, 9, e96637.
- Zhang, Z., & Wood, W. I. (2003). A profile hidden markov model for signal peptides generated by hmmer. *Bioinformatics*, 19, 307–308.

SUPPORTING INFORMATION

Additional supporting information may be found online in the Supporting Information section.

How to cite this article: Liedtke HC, Harney E, Gomez-Mestre I. Cross-species transcriptomics uncovers genes underlying genetic accommodation of developmental plasticity in spadefoot toads. *Mol Ecol*. 2021;00:1–15. <https://doi.org/10.1111/mec.15883>